



Spatio-Temporal Variations of the PM_{2.5}/PM₁₀ Ratios and Its Application to Air Pollution Type Classification in China

Hao Fan, Chuanfeng Zhao*, Yikun Yang and Xingchuan Yang

State Key Laboratory of Earth Surface Processes and Resource Ecology, and College of Global Change and Earth System Science, Beijing Normal University, Beijing, China

OPEN ACCESS

Edited by:

Pasquale Sellitto,
UMR7583 Laboratoire inter-
universitaire des systèmes
atmosphériques (LISA), France

Reviewed by:

Qianqian Zhang,
National Satellite Meteorological
Center (NSMC), China
Jing Li,
Peking University, China

*Correspondence:

Chuanfeng Zhao
czhao@bnu.edu.cn

Specialty section:

This article was submitted to
Atmosphere and Climate,
a section of the journal
Frontiers in Environmental Science

Received: 08 April 2021

Accepted: 01 June 2021

Published: 14 June 2021

Citation:

Fan H, Zhao C, Yang Y and Yang X
(2021) Spatio-Temporal Variations of
the PM_{2.5}/PM₁₀ Ratios and Its
Application to Air Pollution Type
Classification in China.
Front. Environ. Sci. 9:692440.
doi: 10.3389/fenvs.2021.692440

Particulate Matter (PM) is an important indicator of the degree of air pollution. The PM type and the ratio of coarse and fine PM particles determine the ability to affect human health and atmospheric processes. Using the observation data across the country from 2015 to 2018, this study investigates the distribution and proportion of PM_{2.5} and PM₁₀ at different temporal and spatial scales in mainland China; clarifies the PM_{2.5}, PM₁₀ and PM_{2.5}/PM₁₀ ratios interrelation; and classifies the dust, mixed, and anthropogenic type aerosol. It shows that the annual average concentration of PM_{2.5} and PM₁₀ decreased by 10.55 and 8.78 $\mu\text{g m}^{-3}$ in 4 years. PM_{2.5}, PM₁₀, and PM_{2.5}/PM₁₀ ratios show obvious while different seasonal variations. PM_{2.5} is high in winter and low in summer, while PM₁₀ is high in winter and spring, and low in summer and autumn. Differently, the PM_{2.5}/PM₁₀ ratios are the highest in winter, and the lowest in spring. PM_{2.5}/PM₁₀ ratios show strong independence on PM_{2.5} and PM₁₀, implying that it can provide extra information about the aerosol pollution such as aerosol type. A classification method about air pollution types is then further proposed based on probability distribution function (PDF) morphology of PM_{2.5}/PM₁₀ ratios. The results show that dust type mainly lies in the west of Hu-Line, mixed type pollution distributes near Hu-Line, and the anthropogenic type dominates over North China Plain and cities in southern China. The results provide insights into China's future clean air policy making and environmental research.

Keywords: particulate matter, air pollution, PM_{2.5}/PM₁₀ ratios, China, pollution type

HIGHLIGHTS

- 1) PM_{2.5}/PM₁₀ ratios are decreasing year by year and the seasonal variation is obvious from 2015 to 2018.
- 2) PM_{2.5}/PM₁₀ ratios are independent on PM concentration and provides extra aerosol type information.
- 3) An urban pollution classification method based on PM_{2.5}/PM₁₀ ratios is proposed in this study.
- 4) The Hu-line is found as the good dividing line between dust and anthropogenic type aerosol pollution.

INTRODUCTION

Due to its severe impact on human health and significant atmospheric visibility reduction, Particulate Matter (PM) has attracted increasing attention worldwide (Lelieveld et al., 2015; Gu

et al., 2016; An et al., 2019; Zhang et al., 2019; Zhao et al., 2020). The source and composition of PM in the atmosphere are complex, which may be generated directly by the emission sources, or generated by the secondary conversion (Zhao et al., 2018a; Tan et al., 2019). Associated with the different meteorological conditions, the size and composition of PM in the atmosphere vary widely, and could cause various health hazards and weather and climate effects over different locations (Huang et al., 2014; Lelieveld et al., 2015; Liao et al., 2015; Wang et al., 2015; Zhao et al., 2017).

The PM is mainly classified based on the aerodynamic diameter. For example, PM_{2.5} and PM₁₀ refer to particles with aerodynamic diameters less than or equal to 2.5 and 10 μm , respectively. PM_{2.5} is also called fine particles, while PM₁₀ is composed of PM_{2.5} and PM_{2.5-10}. Particles between 2.5 and 10 μm are mainly from natural sources, such as desert, while they may also be caused by human activities, such as road dust and industrial emissions (Gu et al., 2016; Zhou et al., 2016; Chen et al., 2017; Tian et al., 2018). In contrast, PM_{2.5} mainly comes from the combustion of fossil fuels, such as industrial coal combustion, motor vehicle exhaust, and so on (Zhang et al., 2019; Zhao et al., 2019; Fan et al., 2020). From the perspective of physical characteristics, coarse particles can be removed from the atmosphere quickly through dry and wet deposition, while fine particles have a longer life in the atmosphere. Correspondingly, the fine particles are more difficult to control. Also, fine particles are more harmful to humans due to their fine sizes (Kong et al., 2016; Zhou et al., 2016; Talbi et al., 2018; Hvidtfeldt et al., 2019). Understanding the proportion of fine particles in the atmosphere is important for air pollution control and related researches.

Because coarse particles (PM_{2.5-10}) and fine particles (PM_{2.5}) have different physical and chemical characteristics, the proportion of PM_{2.5} to PM₁₀ could provide important extra information about the aerosol pollution, which is worthy to characterize. Actually, previous studies have found that the PM_{2.5}/PM₁₀ ratios can provide a series of important information such as the cause of pollution, the air pollution process, and the impact on life and health (Chu et al., 2015; Wang et al., 2015; Wu et al., 2015; Xu et al., 2017). Generally, a lower PM_{2.5}/PM₁₀ ratio indicates coarse particles dominant, which is more attributed to natural sources (Wang et al., 2015; Zhou et al., 2016; Tian et al., 2018). In contrast, higher PM_{2.5}/PM₁₀ ratios indicate that the air pollution is more from anthropogenic sources (Chu et al., 2015; Kong et al., 2017; Zhao et al., 2018a; Zhao et al., 2019; Fan et al., 2020). Previous studies found that the average PM_{2.5}/PM₁₀ ratios observed were 0.62 in Wuhan, and 0.54 and 0.44 in Beijing in winter and spring, respectively (Kong et al., 2016; Xu et al., 2017). In Europe with a higher level of urbanization, the PM_{2.5}/PM₁₀ ratios are between 0.39 and 0.74, with the lowest values occurring in Southern Europe and the highest values occurring in Eastern Europe (Eeftens et al., 2012). A regional study of mixed agricultural and industrial development in the state of São Paulo, Brazil showed that the PM_{2.5}/PM₁₀ ratios were in the range of 0.33–0.47 (Franzin et al., 2020). In Saudi Arabia in the Middle East, which is obviously affected by the desert and arid climate, the PM_{2.5}/PM₁₀ ratios are 0.25–0.52, and the average value is only 0.3 (Khodeir et al., 2012).

Therefore, the PM_{2.5}/PM₁₀ ratios are affected by multiple factors such as the underlying surface, human activities, and meteorological conditions, resulting in large spatio-temporal variations (An et al., 2019; Zhang et al., 2019; Fan et al., 2020).

In China, air pollution has become one of the studies focus during recent years (Yang et al., 2016; Ding et al., 2017; Shi et al., 2018; Zhao et al., 2018b; Sweerts et al., 2019; Yang et al., 2019; Zhang et al., 2019; Zhao et al., 2019). On one hand, PM pollution is severe in China, attracting a lot of attentions from the public. On the other hand, China has begun to reduce emissions significantly since 2013 (Zhang et al., 2019; Fan et al., 2020). Regardless of the application of remote sensing products, ground observation data, or model simulations, PM, especially PM_{2.5}, is often the most important air pollutant that is frequently studied. However, the related researches on the PM_{2.5}/PM₁₀ ratios are still insufficient until today, especially for their spatial distribution characteristics and temporal variations at national scale. A small number of existing researches have mainly focused on the short-term observation results at typical cities such as Beijing and Wuhan (Kong et al., 2016; Xu et al., 2017), or have used very limited ground-based remote sensing observations to represent regional features (Wang et al., 2015; Wu et al., 2015). In fact, China's population and industry are highly unevenly distributed, and the temporal and spatial differences in air pollution are large. Therefore, it is highly demanded to investigate the spatial and temporal variations of PM_{2.5}/PM₁₀ ratios at national scale. In addition, classifying the changes of PM_{2.5}/PM₁₀ ratios can more effectively characterize the underlying atmospheric processes at regional scale (Chu et al., 2015; Wang et al., 2015; Talbi et al., 2018).

In order to fully understand the changes of air pollution in China and then make reliable policies to control air pollution, this study aims to quantify the PM_{2.5}, PM₁₀, PM_{2.5}/PM₁₀ ratios by using the ground observation data from 367 cities across the country between 2015 and 2018, to reveal their differences in spatial and temporal changes, and to propose a method to classify the air pollution types over various regions based on PM_{2.5}/PM₁₀ ratios.

DATA AND METHODS

Study Area

China has a vast territory, with a north-south and east-west span of more than 5,000 km, and pollution has significant changes with time and space. In this study, we carry out the variation analysis of air pollutants at two spatial scales. One is the analysis of PM_{2.5}, PM₁₀, PM_{2.5}/PM₁₀ ratios in 367 cities across mainland China (Figure 1). The other is the analysis of PM_{2.5}, PM₁₀, PM_{2.5}/PM₁₀ ratios by dividing all stations into 31 provincial-level administrative units for their spatial difference comparison and regional feature.

Data

The research period of this study is from January 1, 2015 to December 31, 2018. The PM_{2.5} and PM₁₀ observation at national

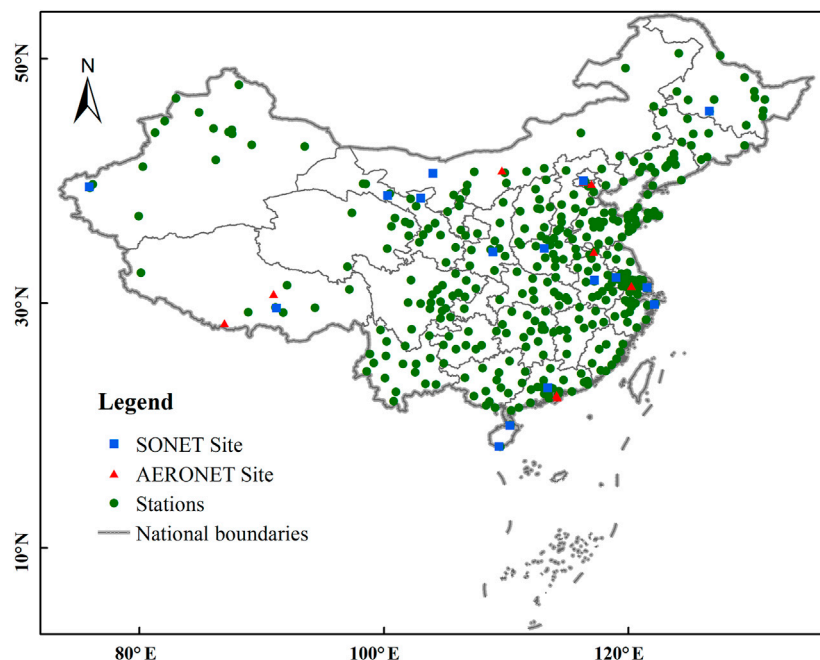


FIGURE 1 | The spatial map about the study area and observation stations, along with the sites used for evaluation of our study results, which are SONET sites and AERONET sites.

stations in each city is operated by the Ministry of Ecology and Environment of the People's Republic of China, and the data are released on the website (<http://www.mee.gov.cn/>) of the China Ministry of Ecology and Environment in real-time.

At this stage, Aerosol Optical Depth (AOD) can be obtained from both ground-based and satellite based remote sensing. As shown in **Figure 1**, ground-based remote sensing of AOD used in this study was obtained from Aerosol Robotic Network (AERONET, <https://aeronet.gsfc.nasa.gov/>). This data was obtained through a multi-band solar photometer (CE-318). AERONET has accumulated a large amount of AOD data worldwide, with long time series and high accuracy, and is widely used as a standard for satellite inversion accuracy verification. In addition, this study takes use of atmospheric aerosol optical, physical, chemical, and radiation characteristics data obtained from long-term observations of the Solar-Sky Radiometer Observation Network (SONET, <http://www.sonet.ac.cn>) of the Chinese Academy of Sciences (Li et al., 2018; Li et al., 2019). It should be noted that the AOD data is not separately analyzed and calculated in this study, but is mainly used for comparison of results in the discussion.

$PM_{2.5}/PM_{10}$ ratio can provide information about the aerosol particle size distribution, based on which we would propose a method to classify aerosol types by setting up some threshold values. As shown later in *Aerosol Type Classification Method Using $PM_{2.5}/PM_{10}$ Ratios* section, one variable we mainly take use for aerosol type classification is the PDF distribution of $PM_{2.5}/PM_{10}$ ratios (Markonis et al., 2019), and the specific formula is as follows,

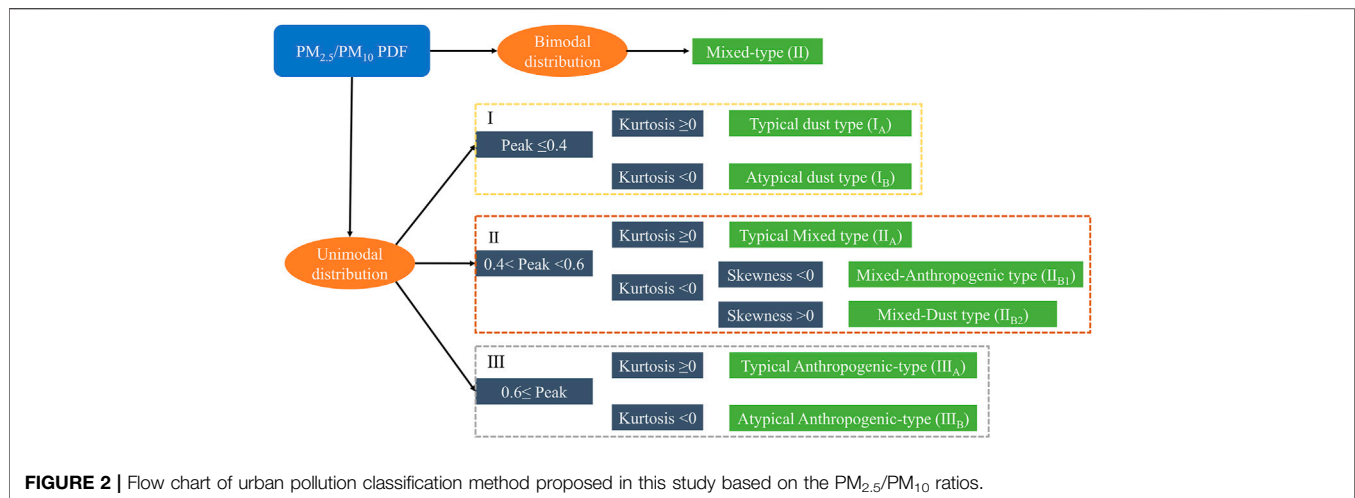
$$P(a \leq x \leq b) = \int_a^b f_X(x) dx \quad (1)$$

where $P(a \leq x \leq b)$ is the probability of occurrence for $PM_{2.5}/PM_{10}$ ratios with values between a and b , and $f_X(x)$ is frequency of occurrence of $PM_{2.5}/PM_{10}$ ratios at a specific value of x between a and b .

Aerosol Type Classification Method Using $PM_{2.5}/PM_{10}$ Ratios

In this study, we proposed the aerosol type classification method based on the spatiotemporal analysis of $PM_{2.5}/PM_{10}$ ratios. As indicated earlier, the classification takes use of the PDF of $PM_{2.5}/PM_{10}$ ratios, along with the skewness and kurtosis of related variables. Skewness is a measure of the direction and degree of skew of statistical data distribution, and is a numerical feature of the degree of asymmetry of statistical data distribution. The skewness includes normal distribution (Skewness = 0), right skewed distribution (Skewness > 0), and left skewed distribution (Skewness < 0). Kurtosis is a characteristic number that represents the peak value of PDF at the average value. Generally speaking, Kurtosis > 0 represents a peak distribution, and Kurtosis < 0 indicates a flat distribution (Fu and Pawlowski, 2016; Cain et al., 2017; Mei et al., 2017).

The specific classification methods are shown in **Figure 2**. First, we list the PDF of $PM_{2.5}/PM_{10}$ ratios at all stations, which are shown in **Supplementary Figures S1–S5**. Second, we analyze the PDF distribution type to examine whether it is unimodal or



bimodal distribution. If the PDF is a bimodal distribution, the aerosol particle type at this site is **preliminarily judged** as a mixed type (type II). These cities include Shaoxing, Urumqi, Karamay, Xishuangbanna, Changji and Wujiaqu. Third, we further **examine the range of peaks** at all stations **showing a single-peak distribution**. The aerosol particles with PDF peak value < 0.4 are classified as dust type (type I); with PDF peak value ranging from 0.4 to 0.6 are classified as the mixed type (type II); and those with PDF peak value > 0.6 are classified as the anthropogenic type (type III). Fourth, **according to the Kurtosis** of the PDF distribution at each site, **we determine whether the aerosols belong to the typical category** under this broad category. If kurtosis ≥ 0 , it means that the site's PDF distribution is concentrated, which is a typical category of the type; if kurtosis < 0 , it means that the site's PDF distribution is flat, which is an atypical category of the type. For example, when kurtosis ≥ 0 , the dust type aerosol is classified as the typical dust type (type I_A), otherwise it is the atypical dust type (type I_B). Fifth, considering that the **atypical mixed type is relatively complex**, we further judged the type II_B according to Skewness. When Skewness < 0 , it indicates that the site belongs to the mixed type that is more polluted by anthropogenic; and when Skewness > 0 , it belongs to the mixed type that is more polluted by dust. It should be noted that **although the selection of 0.4 and 0.6 as the classification criteria is subjective to a certain degree**, it is **consistent with the classification results** of urban pollution types in previous studies (Wang et al., 2015; Xu et al., 2017; Tian et al., 2018). In addition, every 0.1 change in the threshold will cause approximately 3.8–7.1% of urban aerosol types to change.

Cities classified according to this method can be summarized into three major categories of dust type (I), mixed type (II), and anthropogenic type (III), and seven small categories of typical dust type (I_A) and atypical dust type (I_B), typical mixed type II_A, mixed-anthropogenic type (II_{B1}) and mixed-dust type (II_{B2}), typical anthropogenic type (III_A) and atypical anthropogenic type (III_B) (Figures 2, 3). Figure 3 shows the PDF distributions over seven typical cities for each small category. These cities are located in the regions of Qinghai-Tibet Plateau

(Xining), North China (Shijiazhuang, Hohhot), Northwest China (Hetian), East China (Jiaxing, Huzhou) and Central China (Yiyang). Thus, the cities have their typical region representative. Figure 3 also shows the differences in coarse and fine aerosol particles among these regions. Based on this classification method, we can quantitatively separate various types of air pollution, which will be described in detail in *Air Pollution Classification* section.

RESULTS AND DISCUSSION

Variation Characteristics of $PM_{2.5}$, PM_{10} and $PM_{2.5}/PM_{10}$ Ratios

From 2015 to 2018, the **annual average mass concentrations of $PM_{2.5}$ and PM_{10}** at all sites in China **showed a decreasing trend** (Figure 4). The average annual mass concentrations of $PM_{2.5}$ in the 4 years are 48.63, 45.00, 42.91, and 38.08 $\mu g m^{-3}$, and that for PM_{10} are 85.13, 80.77, 78.76 and 74.37 $\mu g m^{-3}$ respectively. According to the China ambient air quality standards GB3095-2012 (<http://www.mee.gov.cn/>), the **annual average concentration limits** of $PM_{2.5}$ and PM_{10} for good air quality are 35 and 70 $\mu g m^{-3}$, respectively. As a result, the annual average concentration of $PM_{2.5}$ **exceeded the standard** by 38.9 and 8.8% in 2015 and 2018, respectively; and the annual average concentration of PM_{10} **exceeded the standard** by 21.6 and 6.2% in 2015 and 2018, respectively. Same as the findings from previous studies (Wang et al., 2015; Zhang et al., 2019; Fan et al., 2020), $PM_{2.5}$ has been the focus of air pollution control since 2013, so the rate of its decline has been faster than other air pollutants. Although PM_{10} declined more slowly, it is closer to the limit of air quality standards than $PM_{2.5}$. While there is a decreasing trend, PM in the winter of 2016/2017 has not decreased significantly, as shown in Figure 4. This is because two large-scale severe haze events occurred in northern China at that time in winter, which even reached the highest level of air quality warning degree in China (An et al., 2019). The annual average change of $PM_{2.5}/PM_{10}$ ratios was similar as the change of $PM_{2.5}$ and PM_{10} concentrations, and decreased from 0.57 in 2015

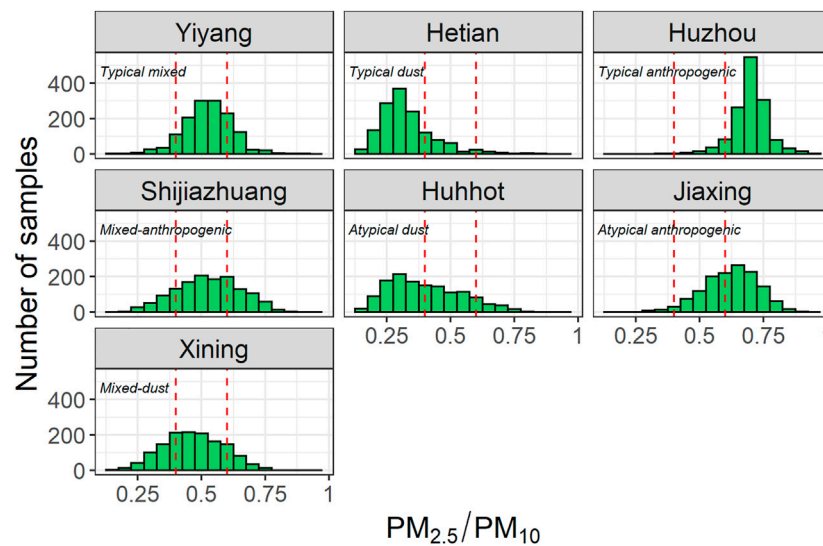


FIGURE 3 | Schematic PDF distribution of $PM_{2.5}/PM_{10}$ ratios for seven types of urban pollution. The red dotted lines indicate the $PM_{2.5}/PM_{10}$ ratios of 0.4 and 0.6, respectively.

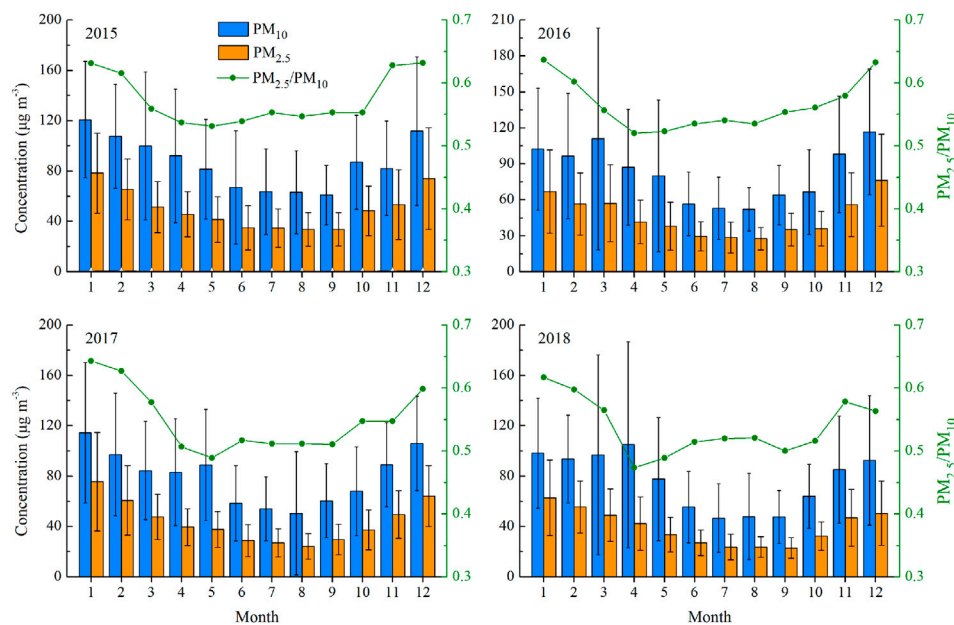


FIGURE 4 | The monthly variation of average PM concentrations ($PM_{2.5}$ and PM_{10}) and $PM_{2.5}/PM_{10}$ ratios obtained from all national stations in 2015, 2016, 2017 and 2018.

to 0.54 in 2018, which suggests that the proportion of fine PM in China is also slowly decreasing.

Figure 4 also shows the monthly changes of $PM_{2.5}$, PM_{10} and $PM_{2.5}/PM_{10}$ ratios during the study period. The monthly average $PM_{2.5}$ has a clear seasonal variation in each year, high in winter and low in summer. This seasonal distribution of $PM_{2.5}$ is associated with the combined effects of anthropogenic

emissions and meteorology (Chu et al., 2015; An et al., 2019; Sun et al., 2019; Zhao et al., 2019; Fan et al., 2020). The relatively large amount of pollutant emissions in winter determine the high level of air pollution, and the meteorological conditions with more stable atmospheric status and less wet deposition are unfavorable for diffusion and removal of air pollutants in winter (Wang et al., 2015; Xu et al., 2017). PM_{10} is higher in

winter and spring, especially in 2016 and 2018. The highest monthly average PM_{10} values appeared in March and April, with the largest standard deviation in spring. This suggests that the PM_{10} is more from natural sources (such as sandstorm), and the emission reduction treatment may only be effective for coarse particles emitted from anthropogenic sources (Khodeir et al., 2012; Chen et al., 2017; Yuan et al., 2019).

The seasonal variation of monthly average $PM_{2.5}/PM_{10}$ ratios is not completely consistent with that of $PM_{2.5}$ and PM_{10} . The highest $PM_{2.5}/PM_{10}$ ratio values occur in winter and the lowest values occur in April and May. The occurrence of the low $PM_{2.5}/PM_{10}$ ratio values may be directly related to the high values of PM_{10} from dust in spring. The $PM_{2.5}/PM_{10}$ ratios have very gentle variation from April to October in each year, with values about 0.55 in 2015–2016 and about 0.5 in 2017–2018. This also suggests that the monthly average of $PM_{2.5}/PM_{10}$ ratios in China has slightly declined for recent years, but the weak monthly variation pattern from spring to autumn remains basically unchanged.

We visualize the $PM_{2.5}/PM_{10}$ ratios at each site in the national map in four seasons (Figure 5) and find that the spatial distributions of $PM_{2.5}/PM_{10}$ ratios among the four seasons are significantly different. Almost at all stations there are the highest $PM_{2.5}/PM_{10}$ ratios in winter, and the $PM_{2.5}/PM_{10}$ ratios in the cities east of “Hu-Line” and the northern Xinjiang region in winter all reach above 0.6. As indicated earlier, this seasonal variation may be related to more emission in winter than in other seasons from the coal-fired heating and industrial activities in these areas, along with the more unfavorable meteorological conditions for diffusion (Huang et al., 2014; An et al., 2019). In the southern region, the humidity is relatively high in winter, and particle hygroscopic growth will further increase the proportion of fine particles (Xu et al., 2017; Zhao et al., 2018a; Yang et al., 2019). Therefore, the current “Hu-Line” still has a certain indicating significance not only for the speed of China’s economic development, but also for the classification of urban air pollution types.

In spring, China inland areas warm up to accelerate air drying with sparse natural vegetation (Fan et al., 2018), and windy weather condition causes sand and dust to travel from northwest China to the coast (Chen et al., 2017; Yuan et al., 2019), which results in high PM_{10} and low $PM_{2.5}/PM_{10}$ ratios in more cities in spring. The contrast is obvious at the Qinling Mountains—Huaihe River Line, in which the $PM_{2.5}/PM_{10}$ ratio is higher in the south with values almost all above 0.55, and lower in the north with values almost all below 0.5 except for a few cities in the northeast. We also find that the $PM_{2.5}/PM_{10}$ ratios in cities in the southern region are higher than that in northern regions in all four seasons, which implies that although there is more serious air pollution in north China regions such as the North China Plain and Fenwei Plain, the proportion of fine particles is higher in south China region.

In summary, the seasonal changes in the ratio of $PM_{2.5}/PM_{10}$ are mainly due to changes in anthropogenic emission and meteorological conditions in different seasons. Specifically, the higher ratio of $PM_{2.5}/PM_{10}$ in winter was mainly caused by higher emissions from heating and more stagnant weather conditions

(Wang et al., 2015). On the contrary, more precipitation in summer and more sandstorms in spring result in a relatively low ratio of $PM_{2.5}/PM_{10}$ (Wang et al., 2015; Fan et al., 2020). Combined with previous studies (Zhang et al., 2019; Fan et al., 2020), the year-to-year decrease in the $PM_{2.5}/PM_{10}$ ratio found in this study should be mainly caused by rigid air quality control policies and emission reduction measures in recent years. As for the difference in the ratio of $PM_{2.5}/PM_{10}$ between regions, it is closely related to the effectiveness of governance, meteorology, and the background value of local pollution. For example, the North China has a relatively high PM_{10} due to the impact of dust, while southern China is more susceptible to the impact of monsoon precipitation, resulting in relatively low PM_{10} .

Spatial Variation Analysis of $PM_{2.5}/PM_{10}$ Ratios

We analyze the spatial distribution of $PM_{2.5}/PM_{10}$ ratios in 31 provinces along with the annual average of $PM_{2.5}$ concentration in each province from 2015 to 2018, which is shown in Figure 6. Each column in Figure 6 represents the relative difference of annual average $PM_{2.5}/PM_{10}$ ratio at each province compared with the national average in every year from 2015 to 2018, which provides information about the spatial change of the fine particle proportion in 31 provinces. The high-value areas are mainly concentrated in the provinces in the North China Plain and surrounding provinces as well as Xinjiang Autonomous, which is consistent with the findings from previous studies (Huang et al., 2014; Fan et al., 2020).

Figure 6 shows that $PM_{2.5}/PM_{10}$ ratios in Xinjiang, Tibet, Gansu, Inner Mongolia, Ningxia, Qinghai, and Hainan are far lower than the national average. All of these provinces are inland provinces in northwestern China except Hainan, with no obvious inter-annual changes of $PM_{2.5}/PM_{10}$ ratios during the study period. The $PM_{2.5}/PM_{10}$ ratios in the three northeast provinces are close to the national average. The four-year averages of $PM_{2.5}/PM_{10}$ ratios in Heilongjiang and Liaoning are lower than the national averages by 1.4 and 0.6%, respectively. In Jilin province, the $PM_{2.5}/PM_{10}$ ratios show a decreasing trend during the study period compared to the national averages, with values from 4.2% higher in 2015 to 0.7% lower than the national average in 2018. Except for Yunnan and Hainan provinces in southern China, the $PM_{2.5}/PM_{10}$ ratios in all other provinces have increasing trends during the study period compared to the national averages. Among them, Shanghai is the province with the highest $PM_{2.5}/PM_{10}$ ratios in the country for each year during the study period, with an average value of 19.6% higher than the national average during the four years. The proportions of fine particles to total in Sichuan, Chongqing, Guizhou, Guangxi, Guangdong, Hunan, Fujian and Jiangsu show increasing trends to varying degrees relatively to the national average. The changes of $PM_{2.5}/PM_{10}$ ratios in the northern and central provinces where air pollution is severe are even more complicated. $PM_{2.5}/PM_{10}$ ratios in Hebei, Shanxi, Shandong, and Shaanxi are lower than the national average, while Henan Province fluctuates between -1.8% below the national average and 2.2% above the national average. The $PM_{2.5}/PM_{10}$ ratios in

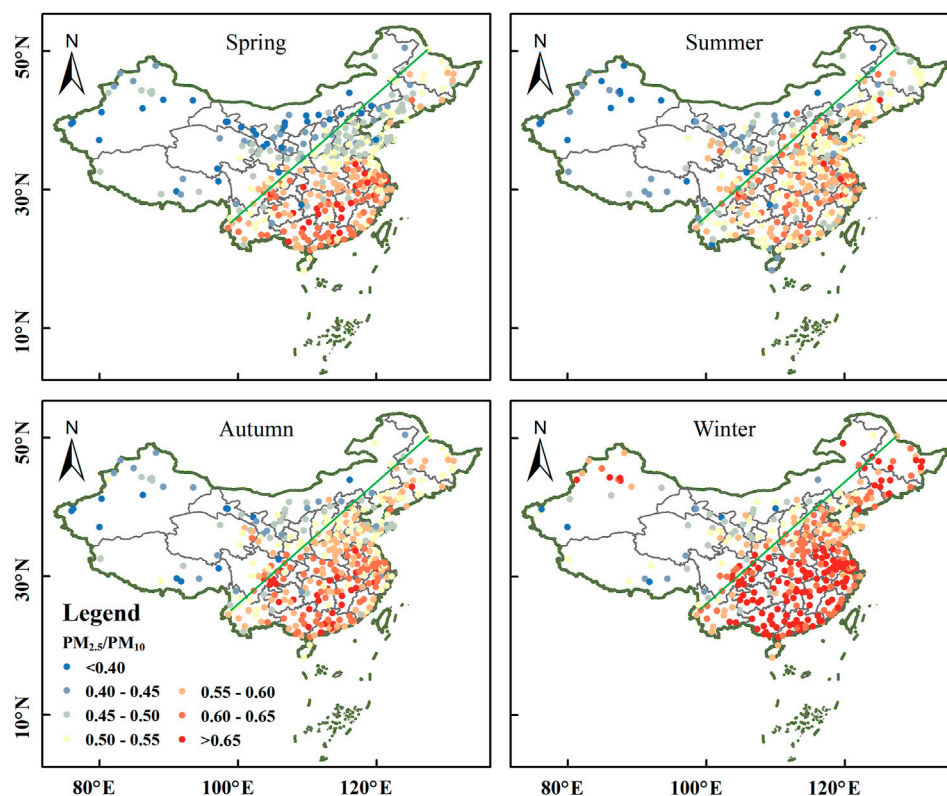


FIGURE 5 | The spatial distributions of averaged $PM_{2.5}/PM_{10}$ ratios at national sites in China for four seasons of spring, summer, autumn and winter during the study period from 2015 to 2018. The green line represents the Hu-line.

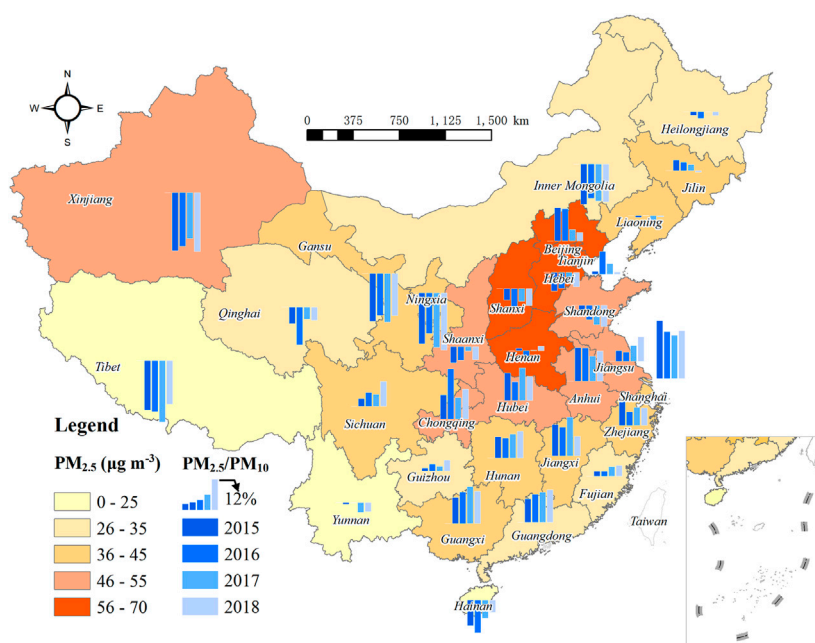


FIGURE 6 | The spatial distribution of $PM_{2.5}/PM_{10}$ ratios in 31 provinces along with the annual average of $PM_{2.5}$ concentration in each province from 2015 to 2018.

Beijing and Tianjin have fallen rapidly compared to the national averages, decreasing by 9.9 and 8.3% respectively in four years. The results shown here also suggest that there is no clear relationship between the temporal variations of $PM_{2.5}$ concentrations and $PM_{2.5}/PM_{10}$ ratios in each province. **Table 1** further visually shows the changes in the ratio of $PM_{2.5}/PM_{10}$ in each province from 2015 to 2018, and whether it is significantly different from the national average. It clearly shows that the ratio of $PM_{2.5}/PM_{10}$ in each province is basically a downward trend from 2015 to 2018, which reflects the efficiency of air pollution control. Moreover, the ratio of $PM_{2.5}/PM_{10}$ in some provinces in southern China, such as Guangdong, Guangxi, and Jiangxi, is significantly higher than the national average, while provinces in northern China, such as Gansu, Ningxia, and Inner Mongolia, have the opposite result.

$PM_{2.5}/PM_{10}$ ratios could provide the pollution source information (such as natural or anthropogenic sources) to some extent. As shown in **Figures 7, 8**, the $PM_{2.5}/PM_{10}$ ratios can serve as an extra indicator in addition to $PM_{2.5}$ or PM_{10} , and provide information about the aerosol types. $PM_{2.5}/PM_{10}$ ratios have no significant correlations with $PM_{2.5}$ and PM_{10} , as shown in **Figures 7A,B**. In contrast, **Figure 7C** has shown that $PM_{2.5}$ and PM_{10} have a good linear relationship at the provincial level with R^2 between 0.65 and 0.76, which passes the significance test ($p < 0.001$). This high correlation is consistent with the findings from previous researches (Wang et al., 2015; Kong et al., 2016; Talbi et al., 2018). In order to investigate the potential effects from different spatial scales, we also perform an analysis based on 367 site observations, which is shown in **Figure 8**. **Figure 8A** shows that the fitting trend of $PM_{2.5}/PM_{10}$ ratios and $PM_{2.5}$ is almost parallel to the X axis, and the correlation is extremely low ($0 < R^2 < 0.04$). Although $PM_{2.5}/PM_{10}$ ratios and PM_{10} have a negative linear relationship, the correlation is also low ($0.07 < R^2 < 0.21$) as shown in **Figure 8B**. The negative relationship between $PM_{2.5}/PM_{10}$ ratios and PM_{10} is mainly due to a small amount of PM_{10} observations with concentrations greater than $175 \mu g m^{-3}$, which makes this relationship highly unreliable. In contrast, **Figure 8C** shows that $PM_{2.5}$ and PM_{10} have a good linear correlation by using site observations with R^2 between 0.64 and 0.79 ($p < 0.001$). In addition, it is found that the relationships found in **Figure 8** vary little with time of year during the study period. All of these analysis results indicate that $PM_{2.5}/PM_{10}$ ratios can serve as an independent indicator of aerosol pollution.

Air Pollution Classification

We here use hourly $PM_{2.5}/PM_{10}$ ratio data from 367 sites in China during the study period to classify the characteristics of near surface air pollution. The detailed classification method and process have been given in *Aerosol Type Classification Method Using $PM_{2.5}/PM_{10}$ Ratios* section, with the framework shown in **Figure 2**. **Figure 9** shows the results of our classification. As shown, cities classified as sand and dust pollution (type I) are located in the west and north of “Hu-Line”; mixed pollution (type II) cities are mainly located near “Hu-Line,” North China Plain, Yunnan Provinces and some coastal cities; and anthropogenic pollution (type III) cities are almost all located in the southeast of “Hu-Line.”

The desert and Gobi in China are mainly located in the northwest inland region. In addition, the central and western regions of the Inner Mongolia Plateau and the Qinghai-Tibet Plateau together form the main area of the west of the “Hu-Line.” The vegetation coverage is low in the northwest inland region (Chen et al., 2017; Fan et al., 2018; Yuan et al., 2019), and the absolute quantity and proportion of PM_{10} affected by natural sources are relatively high (**Figures 3, 4**). In recent years, the development of capital cities of every province and some industrial cities in northwestern China has increased the proportion of fine particles. Therefore, we found that industrial cities such as Lanzhou-Xining City Group, Urumqi, Yinchuan, and Baotou have shown mixed pollution type of aerosols.

Our analysis finds that in the cities of Sichuan Basin, central China, southern coast, and eastern China, the PM particles are mostly from anthropogenic pollution. The common characteristics of these regions are rapid industrial development, high urbanization rate, and high anthropogenic emissions (Wu et al., 2015; Liu et al., 2018; Xu et al., 2020). At the same time, these areas are far away from the natural sand and dust sources. Correspondingly, the dust particles caused by strong winds in spring in these areas are far less than that in those cities in Northwest and North China. In addition, the overall environmental humidity in the south is higher than that in the north, and the hygroscopic growth of new particles may also increase the proportion of $PM_{2.5}$ (Zhao et al., 2018a; Wang et al., 2020). Therefore, under the combined effect of multiple causes, it appears as a type of anthropogenic pollution in the cities of Sichuan Basin, central China, southern coast, and eastern China. The North China Plain area is more susceptible to dust transport than the South, especially in spring (Chen et al., 2017; Yuan et al., 2019; Fan et al., 2020). Therefore, although the absolute amount of $PM_{2.5}$ concentration in the North China Plain is the highest in the country, the proportion of fine particles is not the highest. This is also an important reason for more mixed pollution in the cities of the North China Plain.

While the PM concentration is found mainly determined by emissions, meteorological factors also play an important role by affecting the diffusion and generation of pollutants. Related studies (Yang et al., 2016; Zhou et al., 2016; Zhao et al., 2019) have shown that wind speed and $PM_{2.5}$ concentration are usually negatively correlated, and if no precipitation occurs, relative humidity (RH) is generally positively correlated with $PM_{2.5}$ concentration. Our research results also found that the ratio of $PM_{2.5}/PM_{10}$ in southern cities in China tends to be higher due to higher RH in winter (**Figure 5**). In this regard, emissions likely play a leading role in the ratio of $PM_{2.5}/PM_{10}$ at long time scale over a region with similar climatology. In contrast, when there is no significant difference in emissions, meteorological factors are more likely to play an important role.

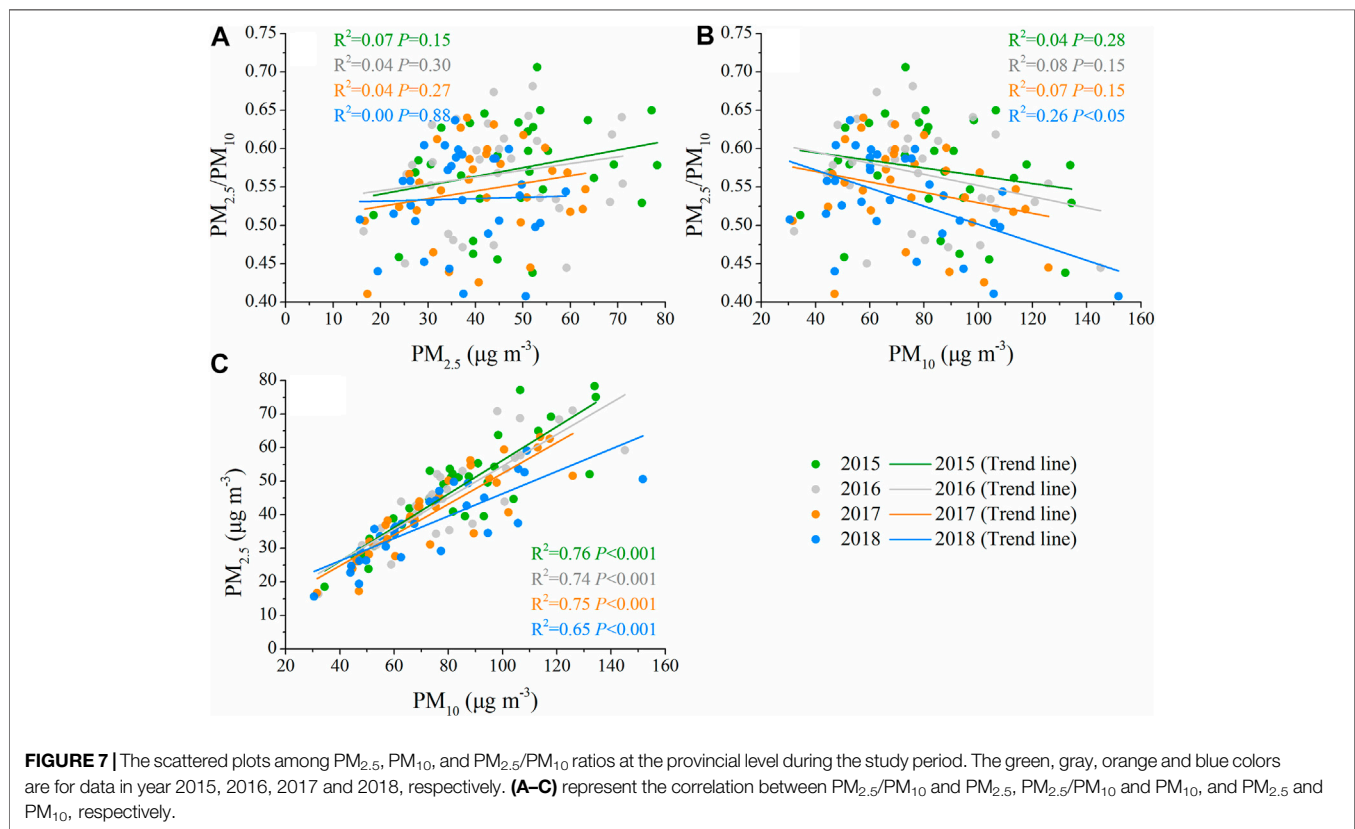
Comparative Discussion and Uncertainty

Based on the analysis in the previous three sections, it can be found that $PM_{2.5}/PM_{10}$ ratios are important in indicating air pollution type and have very weak dependence on either $PM_{2.5}$ or PM_{10} . Currently, there are several studies that classified the “basic

TABLE 1 | The changes in the ratio of PM_{2.5}/PM₁₀ in each province and the country from 2015 to 2018.

Name	PM _{2.5} /PM ₁₀ ratio (mean)				Name	PM _{2.5} /PM ₁₀ ratio (mean)			
	2015	2016	2017	2018		2015	2016	2017	2018
Anhui	0.65 ^a	0.64 ^a	0.60 ^a	0.60 ^a	Liaoning	0.57	0.57	0.54	0.53
Beijing	0.65 ^a	0.64 ^a	0.57	0.55	Neimenggu	0.48 ^a	0.49 ^a	0.46 ^a	0.45 ^a
Fujian	0.58	0.58	0.57	0.56	Ningxia	0.46 ^a	0.47 ^a	0.43 ^a	0.41 ^a
Gansu	0.46 ^a	0.47 ^a	0.44 ^a	0.44 ^a	Qinghai	0.53	0.48 ^a	0.52	0.51
Guangdong	0.63 ^a	0.63 ^a	0.61 ^a	0.60 ^a	Shandong	0.56	0.53	0.50 ^a	0.49 ^a
Guangxi	0.63 ^a	0.64 ^a	0.63 ^a	0.60 ^a	Shanxi	0.55	0.52 ^a	0.52	0.50 ^a
Guizhou	0.58	0.58	0.56	0.56	Shaanxi	0.54	0.54	0.54	0.51
Hainan	0.51 ^a	0.49 ^a	0.51	0.51	Shanghai	0.71 ^a	0.67 ^a	0.64 ^a	0.64 ^a
Hebei	0.53 ^a	0.53	0.52	0.50	Sichuan	0.59	0.60 ^a	0.57	0.59 ^a
Henan	0.58	0.55	0.55	0.54	Tianjin	0.58	0.62 ^a	0.57	0.54
Heilongjiang	0.56	0.55	0.55	0.53	Xizang	0.46 ^a	0.45 ^a	0.41 ^a	0.44 ^a
Hubei	0.64 ^a	0.61 ^a	0.62 ^a	0.59 ^a	Xinjiang	0.44 ^a	0.44 ^a	0.44 ^a	0.41 ^a
Hunan	0.62 ^a	0.61 ^a	0.60 ^a	0.59 ^a	Yunnan	0.57	0.57	0.52	0.52
Jilin	0.60	0.59	0.56	0.53	Zhejiang	0.63 ^a	0.60	0.59 ^a	0.57 ^a
Jiangsu	0.60	0.59	0.58 ^a	0.59 ^a	Chongqing	0.63 ^a	0.68 ^a	0.59 ^a	0.60 ^a
Jiangxi	0.65 ^a	0.63 ^a	0.63 ^a	0.58 ^a	China	0.57	0.57	0.55	0.53

^aindicates that the data passed the significance test ($p < 0.05$).



mode” (Li et al., 2019) and types of regional aerosols in China (Tian et al., 2018) using the ground-based observational data from aerosol remote sensing. However, ground-based aerosol remote sensing observation stations in China are very limited and unevenly distributed, as shown in **Figure 1**. Moreover, the remote sensing observations of aerosol properties generally represent the characteristics of aerosols at high altitudes,

which is difficult or has relatively large uncertainties to represent the aerosol characteristics near surface. Compared with previous studies, this study breaks through the limitations of ground remote sensing sites and develops a nation-scale classification method for the proportion of fine particles, and comprehensively analyzes its environmental indicators (e.g., aerosol types).

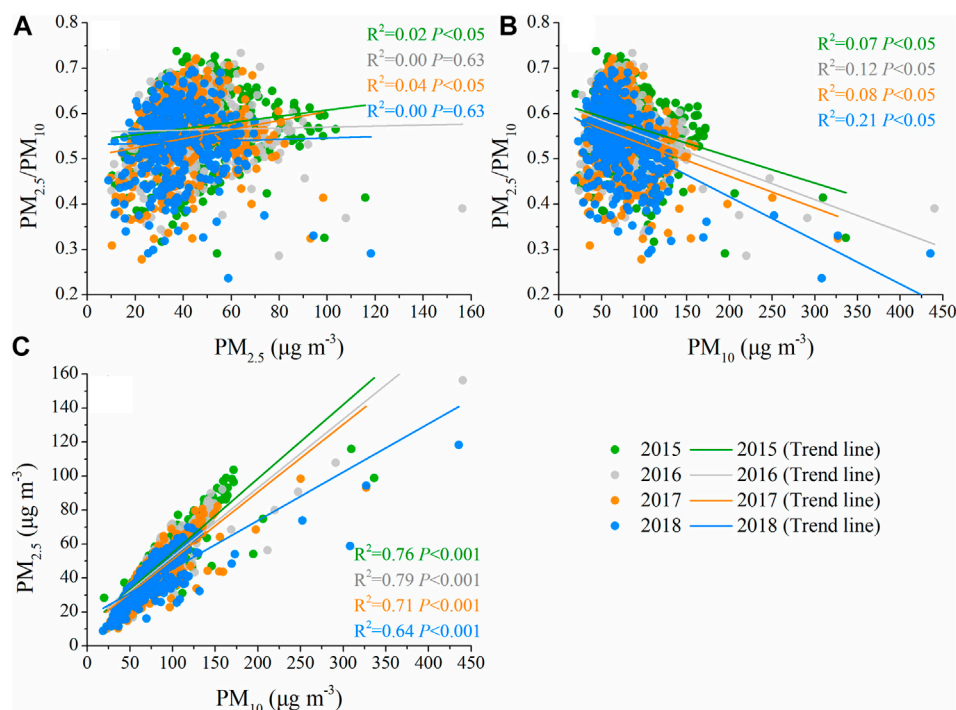


FIGURE 8 | The scattered plots among the $PM_{2.5}$, PM_{10} and $PM_{2.5}/PM_{10}$ ratios obtained from all national ground sites during the study period. The green, gray, orange and blue colors are for data in year 2015, 2016, 2017 and 2018, respectively. **(A–C)** represent the correlation between $PM_{2.5}/PM_{10}$ and $PM_{2.5}$, $PM_{2.5}/PM_{10}$ and PM_{10} , and $PM_{2.5}$ and PM_{10} , respectively.

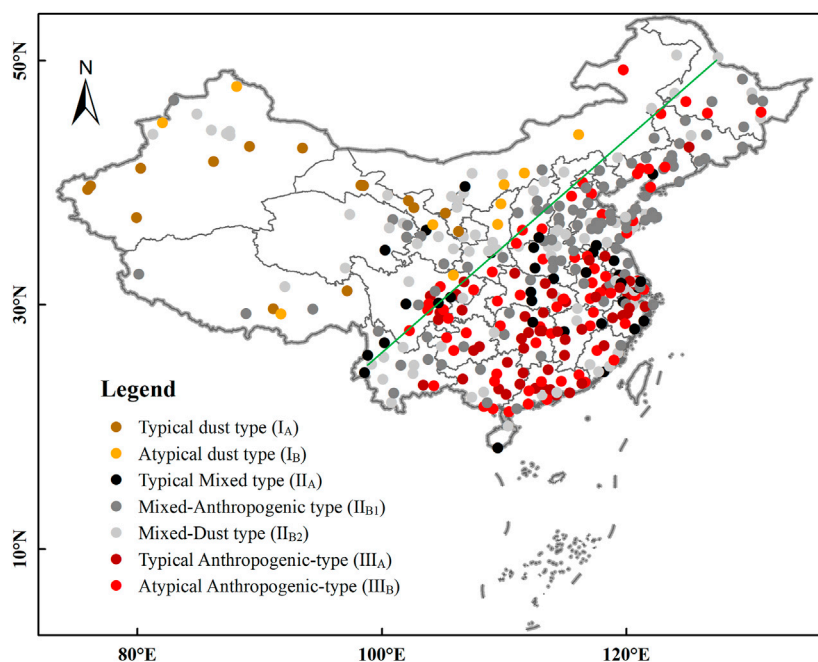


FIGURE 9 | The spatial distribution of urban pollution classification results based on the $PM_{2.5}/PM_{10}$ ratios using our proposed method. The colors represent the seven different classification methods and the green line indicates the Hu-line.

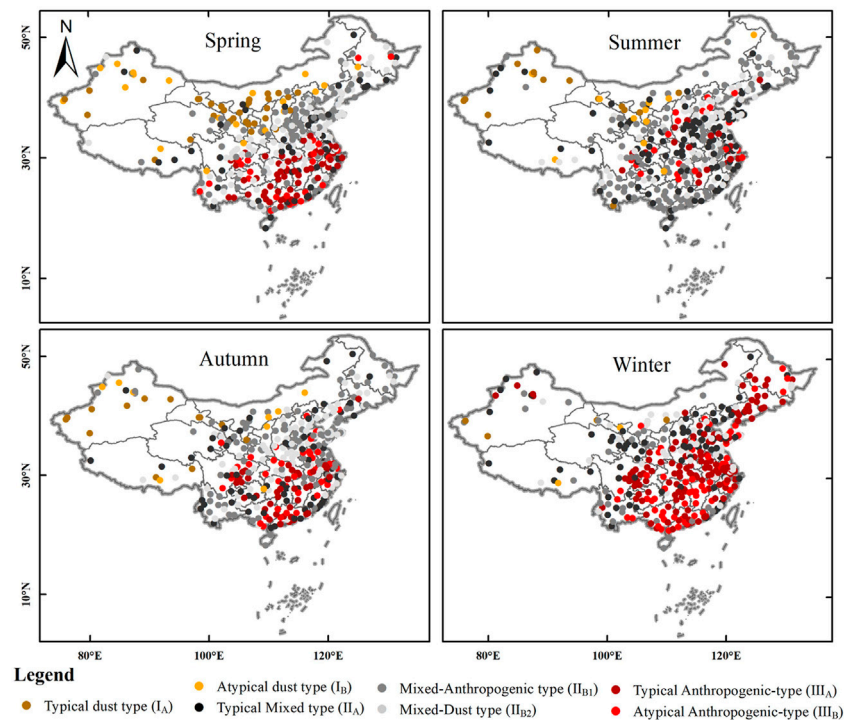


FIGURE 10 | The spatial distribution of urban pollution classification results based on the ratio of $PM_{2.5}/PM_{10}$ in the four seasons.

Our research uses nation-scale ground-based observation data for multi-regional analysis and proposes a reliable aerosol type classification method. Using ground site observations at 24 sites in China, Wang et al. (2015) showed that $PM_{2.5}/PM_{10}$ ratios in western and northeastern cities in China are low, and that in northern and southwestern China are medium, and the highest values are in Yangtze River cities. Differently, we here have analyzed the $PM_{2.5}/PM_{10}$ ratios along with the $PM_{2.5}$ and PM_{10} characteristics using much more ground stations and carried out the analysis from a national perspective with more findings including the aerosol type classification method and aerosol type distributions separated by the Hu-line.

In addition, we also evaluate the results of aerosol type classification based on AERONET site data (Kong et al., 2016; Tian et al., 2018) and aerosol modal division using SONET site data (Li et al., 2018; Li et al., 2019), which shows that the $PM_{2.5}/PM_{10}$ ratios calculated based on ground station observations provide consistent pollution type classification results. Our method is developed based on near-surface observation data, providing valuable aerosol type information of all provinces in mainland China, which is particularly helpful to the air quality control policy making for all provinces. It is very important to note that our current research only focuses on PM data from terrestrial ground observation sites with insufficient consideration of the chemical composition of aerosols. As the results show, there are mixed dust types in some cities in southern China, which are more likely affected by sea salt aerosols. Therefore, uncertainties

could exist and further in-depth analysis for cities close to ocean is necessary in future.

Based on Figure 9, we have further divided the different seasons, and the results are shown in Figure 10. Like the previous analysis, there are more cities with anthropogenic type and dust type in winter and spring, and more cities with mixed type in summer and autumn. At the same time, we found that the ratio of $PM_{2.5}/PM_{10}$ changes all the time, so it is difficult to give a unique type of air pollution in a city. Obviously, the ratio of $PM_{2.5}/PM_{10}$ is constantly changing, so it is difficult to give the only type of air pollution in the city. Even though, our study provides a reference for changes in macroscopic air pollution characteristics.

CONCLUSION

With the $PM_{2.5}$, PM_{10} concentration data from 367 cities, we investigate their temporal trends from 2015 to 2018, and analyze the spatiotemporal features of $PM_{2.5}/PM_{10}$ ratios at country level and provincial level. Moreover, we propose an air pollution type division method and classify the pollution types based on $PM_{2.5}/PM_{10}$ ratios.

During the study period, the concentrations of $PM_{2.5}$ and PM_{10} show a significant declining trend. The annual average value of $PM_{2.5}/PM_{10}$ ratios also decreases year by year, but the change is small. $PM_{2.5}$, PM_{10} and $PM_{2.5}/PM_{10}$ ratios all have obvious monthly and seasonal variations during the study period. Among them, $PM_{2.5}/PM_{10}$ ratios are the highest in winter, the

lowest in spring, and are similar in summer and autumn with little fluctuation.

The PM_{2.5}/PM₁₀ ratios show clear spatial distribution. The PM concentration in southern China is relatively low, but PM_{2.5}/PM₁₀ ratios are higher than the national average, implying the dominance of anthropogenic pollution in the emission sources. Northwest China and North China are affected by more dust aerosols, while air particles in the south are more likely to absorb moisture and grow. Therefore, the PM_{2.5}/PM₁₀ ratios continue to increase from the northwest and north to the south. In China, PM_{2.5} and PM₁₀ have a very good correlation at both the station scale and provincial scale, while PM_{2.5}/PM₁₀ ratios have no significant correlations with PM_{2.5} and PM₁₀. The independence of PM_{2.5}/PM₁₀ ratio on either PM_{2.5} or PM₁₀ indicates that it can serve as another variable to present the air pollution characteristics.

Using multi-year observation data, we propose an air pollution classification method based on PM_{2.5}/PM₁₀ ratios, which classifies the air pollution into three basic types and seven refined types. Roughly, cities classified as sand and dust pollution (basic type I) are located in the west and north of “Hu-Line”; mixed pollution (basic type II) cities are mainly located near “Hu-Line,” North China Plain, Yunnan Provinces and some coastal cities; and anthropogenic pollution (basic type III) cities are almost all located in the southeast of “Hu-Line.” In China, regional aerosol characteristics are very different, and changes in the proportion of fine particles at surface observation stations can provide information about the process of pollution discharge and weather impact. Obviously, our methods and research results provide support to better understand the formation mechanism of air pollution and evaluate its impact on human health, weather and climate.

REFERENCES

- An, Z., Huang, R.-J., Zhang, R., Tie, X., Li, G., Cao, J., et al. (2019). Severe Haze in Northern China: A Synergy of Anthropogenic Emissions and Atmospheric Processes. *Proc. Natl. Acad. Sci. USA* 116 (18), 8657–8666. doi:10.1073/pnas.1900125116
- Cain, M. K., Zhang, Z., and Yuan, K.-H. (2017). Univariate and Multivariate Skewness and Kurtosis for Measuring Nonnormality: Prevalence, Influence and Estimation. *Behav. Res.* 49 (5), 1716–1735. doi:10.3758/s13428-016-0814-1
- Chen, S., Huang, J., Kang, L., Wang, H., Ma, X., He, Y., et al. (2017). Emission, Transport, and Radiative Effects of mineral Dust from the Taklimakan and Gobi Deserts: Comparison of Measurements and Model Results. *Atmos. Chem. Phys.* 17 (3), 2401–2421. doi:10.5194/acp-17-2401-2017
- Chu, H.-J., Huang, B., and Lin, C.-Y. (2015). Modeling the Spatio-Temporal Heterogeneity in the PM₁₀-PM_{2.5} Relationship. *Atmos. Environ.* 102, 176–182. doi:10.1016/j.atmosenv.2014.11.062
- Ding, J., Miyazaki, K., van der A, R. J., Mijling, B., Kurokawa, J.-i., Cho, S., et al. (2017). Intercomparison of NO_x Emission Inventories over East Asia. *Atmos. Chem. Phys.* 17 (16), 10125–10141. doi:10.5194/acp-17-10125-2017
- Eeftens, M., Tsai, M.-Y., Ampe, C., Anwander, B., Beelen, R., Bellander, T., et al. (2012). Spatial Variation of PM_{2.5}, PM₁₀, PM_{2.5} Absorbance and PM_{coarse} Concentrations between and within 20 European Study Areas and the Relationship with NO₂ - Results of the ESCAPE Project. *Atmos. Environ.* 62, 303–317. doi:10.1016/j.atmosenv.2012.08.038
- Fan, H., Zhao, C., and Yang, Y. (2020). A Comprehensive Analysis of the Spatio-Temporal Variation of Urban Air Pollution in China during 2014–2018. *Atmos. Environ.* 220, 117066. doi:10.1016/j.atmosenv.2019.117066

DATA AVAILABILITY STATEMENT

The original contributions presented in the study are included in the article/**Supplementary Material**, further inquiries can be directed to the corresponding author.

AUTHOR CONTRIBUTIONS

CZ coordinated and supervised the project. CZ, HF, YY, and XY contributed to data analysis, research framework design, and writing the first drafts. HF prepared data and completed all figures. CZ revised the manuscript. All co-authors contributed to the interpretation of the results and to the text.

FUNDING

This research was funded by the National Natural Science Foundation of China, grant number 41925022, and 91837204; the National Key R&D Program on Monitoring, Early Warning and Prevention of Major Natural Disasters, grant number 2017YFC1501403; and the State Key Laboratory of Earth Surface Processes and Resources Ecology. The data used in this study is available at the website <http://www.mee.gov.cn/> or by request to HF via fanhao_geo@163.com.

SUPPLEMENTARY MATERIAL

The Supplementary Material for this article can be found online at: <https://www.frontiersin.org/articles/10.3389/fenvs.2021.692440/full#supplementary-material>

- Fan, H., Zhao, W., Daryanto, S., Fu, B., Wang, S., and Wang, Y. (2018). Vertical Distributions of Soil Organic Carbon and its Influencing Factors under Different Land Use Types in the Desert Riparian Zone of Downstream Heihe River Basin, China. *J. Geophys. Res. Atmos.* 123 (14), 7741–7753. doi:10.1029/2018jd028268
- Franzin, B. T., Guizzellini, F. C., de Babos, D. V., Hojo, O., Pastre, I. A., Marchi, M. R. R., et al. (2020). Characterization of Atmospheric Aerosol (PM₁₀ and PM_{2.5}) from a Medium Sized City in São Paulo State, Brazil. *J. Environ. Sci.* 89, 238–251. doi:10.1016/j.jes.2019.09.014
- Fu, W.-j., and Pawlowski, J. M. (2016). Correlating the Skewness and Kurtosis of Baryon Number Distributions. *Phys. Rev. D* 93 (9), 091510. doi:10.1103/PhysRevD.93.091501
- Gu, Y., Xue, Y., De Sales, F., and Liou, K. N. (2016). A GCM Investigation of Dust Aerosol Impact on the Regional Climate of North Africa and South/East Asia. *Clim. Dyn.* 46, 2353–2370. doi:10.1007/s00382-015-2706-y
- Huang, R.-J., Zhang, Y., Bozzetti, C., Ho, K.-F., Cao, J.-J., Han, Y., et al. (2014). High Secondary Aerosol Contribution to Particulate Pollution during Haze Events in China. *Nature* 514 (7521), 218–222. doi:10.1038/nature13774
- Hvidtfeldt, U. A., Sørensen, M., Geels, C., Ketzel, M., Khan, J., Tjønneland, A., et al. (2019). Long-term Residential Exposure to PM_{2.5}, PM₁₀, Black Carbon, NO₂, and Ozone and Mortality in a Danish Cohort. *Environ. Int.* 123, 265–272. doi:10.1016/j.envint.2018.12.010
- Khodeir, M., Shamy, M., Alghamdi, M., Zhong, M., Sun, H., Costa, M., et al. (2012). Source Apportionment and Elemental Composition of PM_{2.5} and PM₁₀ in Jeddah City, Saudi Arabia. *Atmos. Pollut. Res.* 3 (3), 331–340. doi:10.5094/apr.2012.037

- Kong, L., Xin, J., Liu, Z., Zhang, K., Tang, G., Zhang, W., et al. (2017). The PM_{2.5} Threshold for Aerosol Extinction in the Beijing Megacity. *Atmos. Environ.* 167, 458–465. doi:10.1016/j.atmosenv.2017.08.047
- Kong, L., Xin, J., Zhang, W., and Wang, Y. (2016). The Empirical Correlations between PM_{2.5}, PM₁₀ and AOD in the Beijing Metropolitan Region and the PM_{2.5}, PM₁₀ Distributions Retrieved by MODIS. *Environ. Pollut.* 216, 350–360. doi:10.1016/j.envpol.2016.05.085
- Lelieveld, J., Evans, J. S., Fnais, M., Giannadaki, D., and Pozzer, A. (2015). The Contribution of Outdoor Air Pollution Sources to Premature Mortality on a Global Scale. *Nature* 525 (7569), 367–371. doi:10.1038/nature15371
- Li, Z. Q., Xu, H., Li, K. T., Li, D. H., Xie, Y. S., Li, L., et al. (2018). Comprehensive Study of Optical, Physical, Chemical, and Radiative Properties of Total Columnar Atmospheric Aerosols over China: An Overview of Sun-Sky Radiometer Observation Network (SONET) Measurements. *B. Am. Meteorol. Soc.* 99 (4), 739–755. doi:10.1175/bams-d-17-0133.1
- Li, Z., Zhang, Y., Xu, H., Li, K., Dubovik, O., and Goloub, P. (2019). The Fundamental Aerosol Models over China Region: A Cluster Analysis of the Ground-Based Remote Sensing Measurements of Total Columnar Atmosphere. *Geophys. Res. Lett.* 46 (9), 4924–4932. doi:10.1029/2019gl082056
- Liao, H., Chang, W., and Yang, Y. (2015). Climatic Effects of Air Pollutants over China: A Review. *Adv. Atmos. Sci.* 32, 115–139. doi:10.1007/s00376-014-0013-x
- Liu, L., Chen, Y., Wu, T., and Li, H. (2018). The Drivers of Air Pollution in the Development of Western China: The Case of Sichuan Province. *J. Clean. Prod.* 197, 1169–1176. doi:10.1016/j.jclepro.2018.06.260
- Markonis, Y., Papalexou, S. M., Martinkova, M., and Hanel, M. (2019). Assessment of Water Cycle Intensification over Land Using a Multisource Global Gridded Precipitation DataSet. *J. Geophys. Res. Atmos.* 124 (21), 11175–11187. doi:10.1029/2019jd030855
- Mei, D., Liu, J., Ma, F., and Chen, W. (2017). Forecasting Stock Market Volatility: Do Realized Skewness and Kurtosis Help? *Physica A: Stat. Mech. its Appl.* 481, 153–159. doi:10.1016/j.physa.2017.04.020
- Shi, X., Zhao, C., Jiang, J. H., Wang, C., Yang, X., and Yung, Y. L. (2018). Spatial Representativeness of PM 2.5 Concentrations Obtained Using Observations from Network Stations. *J. Geophys. Res. Atmos.* 123, 3145–3158. doi:10.1002/2017JD027913
- Sun, Y., Zhao, C., Su, Y., Ma, Z., Li, J., Letu, H., et al. (2019). Distinct Impacts of Light and Heavy Precipitation on PM 2.5 Mass Concentration in Beijing. *Earth Space Sci.* 6 (10), 1915–1925. doi:10.1029/2019EA000717
- Sweerts, B., Pfenninger, S., Yang, S., Folini, D., van der Zwaan, B., and Wild, M. (2019). Estimation of Losses in Solar Energy Production from Air Pollution in China since 1960 Using Surface Radiation Data. *Nat. Energy* 4 (8), 657–663. doi:10.1038/s41560-019-0412-4
- Talbi, A., Kerchich, Y., Kerbach, R., and Boughedaoui, M. (2018). Assessment of Annual Air Pollution Levels with PM₁, PM_{2.5}, PM₁₀ and Associated Heavy Metals in Algiers, Algeria. *Environ. Pollut.* 232, 252–263. doi:10.1016/j.envpol.2017.09.041
- Tan, W., Li, C., Liu, Y., Meng, X., Wu, Z., Kang, L., et al. (2019). Potential of Polarization Lidar to Profile the Urban Aerosol Phase State during Haze Episodes. *Environ. Sci. Technol. Lett.* 7 (2), 54–59. doi:10.1021/acs.estlett.9b00695
- Tian, P., Zhang, L., Ma, J., Tang, K., Xu, L., Wang, Y., et al. (2018). Radiative Absorption Enhancement of Dust Mixed with Anthropogenic Pollution over East Asia. *Atmos. Chem. Phys.* 18 (11), 7815–7825. doi:10.5194/acp-18-7815-2018
- Wang, H., Wang, Q., Gao, Y., Zhou, M., Jing, S., Qiao, L., et al. (2020). Estimation of Secondary Organic Aerosol Formation during a Photochemical Smog Episode in Shanghai, China. *J. Geophys. Res. Atmos.* 125, e2019JD032033. doi:10.1029/2019JD032033
- Wang, Y. Q., Zhang, X. Y., Sun, J. Y., Zhang, X. C., Che, H. Z., and Li, Y. (2015). Spatial and Temporal Variations of the Concentrations of PM₁₀, PM_{2.5} and PM₁ in China. *Atmos. Chem. Phys.* 15 (23), 13585–13598. doi:10.5194/acp-15-13585-2015
- Wu, F., Wang, W., Man, Y. B., Chan, C. Y., Liu, W., Tao, S., et al. (2015). Levels of PM 2.5/PM 10 and Associated Metal(loid)s in Rural Households of Henan Province, China. *Sci. Total Environ.* 512–513, 194–200. doi:10.1016/j.scitotenv.2015.01.041
- Xu, G., Jiao, L., Zhang, B., Zhao, S., Yuan, M., Gu, Y., et al. (2017). Spatial and Temporal Variability of the PM_{2.5}/PM₁₀ Ratio in Wuhan, Central China. *Aerosol Air Qual. Res.* 17 (3), 741–751. doi:10.4209/aaqr.2016.09.0406
- Xu, X., Huang, G., Liu, L., Guan, Y., Zhai, M., and Li, Y. (2020). Revealing Dynamic Impacts of Socioeconomic Factors on Air Pollution Changes in Guangdong Province, China. *Sci. Total Environ.* 699, 134178. doi:10.1016/j.scitotenv.2019.134178
- Yang, Q., Yuan, Q., Yue, L., Li, T., Shen, H., and Zhang, L. (2019). The Relationships between PM_{2.5} and Aerosol Optical Depth (AOD) in mainland China: About and behind the Spatio-Temporal Variations. *Environ. Pollut.* 248, 526–535. doi:10.1016/j.envpol.2019.02.071
- Yang, X., Zhao, C., Guo, J., and Wang, Y. (2016). Intensification of Aerosol Pollution Associated with its Feedback with Surface Solar Radiation and Winds in Beijing. *J. Geophys. Res. Atmos.* 121, 4093–4099. doi:10.1002/2015JD024645
- Yuan, T., Chen, S., Huang, J., Wu, D., Lu, H., Zhang, G., et al. (2019). Influence of Dynamic and Thermal Forcing on the Meridional Transport of Taklimakan Desert Dust in Spring and Summer. *J. Clim.* 32 (3), 749–767. doi:10.1175/jcli-d-18-0361.1
- Zhang, Q., Zheng, Y., Tong, D., Shao, M., Wang, S., Zhang, Y., et al. (2019). Drivers of Improved PM_{2.5} Air Quality in China from 2013 to 2017. *Proc. Natl. Acad. Sci. USA* 116 (49), 24463–24469. doi:10.1073/pnas.1907956116
- Zhao, B., Wu, W., Wang, S., Xing, J., Chang, X., Liou, K.-N., et al. (2017). A Modeling Study of the Nonlinear Response of fine Particles to Air Pollutant Emissions in the Beijing-Tianjin-Hebei Region. *Atmos. Chem. Phys.* 17, 12031–12050. doi:10.5194/acp-17-12031-2017
- Zhao, C., Li, Y., Zhang, F., Sun, Y., and Wang, P. (2018a). Growth Rates of fine Aerosol Particles at a Site Near Beijing in June 2013. *Adv. Atmos. Sci.* 35 (2), 209–217. doi:10.1007/s00376-017-7069-3
- Zhao, C., Lin, Y., Wu, F., Wang, Y., Li, Z., Rosenfeld, D., et al. (2018b). Enlarging Rainfall Area of Tropical Cyclones by Atmospheric Aerosols. *Geophys. Res. Lett.* 45 (16), 8604–8611. doi:10.1029/2018gl079427
- Zhao, C., Wang, Y., Shi, X., Zhang, D., Wang, C., Jiang, J. H., et al. (2019). Estimating the Contribution of Local Primary Emissions to Particulate Pollution Using High-Density Station Observations. *J. Geophys. Res. Atmos.* 124 (3), 1648–1661. doi:10.1029/2018jd028888
- Zhao, C., Yang, Y., Fan, H., Huang, J., Fu, Y., Zhang, X., et al. (2020). Aerosol Characteristics and Impacts on Weather and Climate over the Tibetan Plateau. *Natl. Sci. Rev.* 7 (3), 492–495. doi:10.1093/nsr/nwz184
- Zhou, X., Cao, Z., Ma, Y., Wang, L., Wu, R., and Wang, W. (2016). Concentrations, Correlations and Chemical Species of PM_{2.5}/PM₁₀ Based on Published Data in China: Potential Implications for the Revised Particulate Standard. *Chemosphere* 144, 518–526. doi:10.1016/j.chemosphere.2015.09.003

Conflict of Interest: The authors declare that the research was conducted in the absence of any commercial or financial relationships that could be construed as a potential conflict of interest.

Copyright © 2021 Fan, Zhao, Yang and Yang. This is an open-access article distributed under the terms of the Creative Commons Attribution License (CC BY). The use, distribution or reproduction in other forums is permitted, provided the original author(s) and the copyright owner(s) are credited and that the original publication in this journal is cited, in accordance with accepted academic practice. No use, distribution or reproduction is permitted which does not comply with these terms.